



## Article

# Assessing Flood Risks in Coastal Plain Cities of Zhejiang Province, Southeastern China

Saihua Huang<sup>1,2</sup>, Weidong Xuan<sup>1,2</sup>, He Qiu<sup>1,2</sup>, Jiandong Ye<sup>3</sup>, Xiaofei Chen<sup>4</sup>, Hui Nie<sup>1,2</sup> and Hao Chen<sup>1,2,\*</sup>

<sup>1</sup> School of Hydraulic Engineering, Zhejiang University of Water Resources and Electric Power, Hangzhou 310018, China; huangsh@zjweu.edu.cn (S.H.); xuanwd@zjweu.edu.cn (W.X.); 2022b20020@stu.zjweu.edu.cn (H.Q.); nieh@zjweu.edu.cn (H.N.)

<sup>2</sup> International Science and Technology Cooperation Base for Utilization and Sustainable Development of Water Resources, Zhejiang University of Water Resources and Electric Power, Hangzhou 310018, China

<sup>3</sup> Tonglu County Jiangnan Irrigation District Project Management Office, Hangzhou 311500, China; tlyjd158@163.com

<sup>4</sup> Zhejiang Water Conservancy Development Planning Research Center, Hangzhou 310012, China; cxf@zjwater.gov.cn

\* Correspondence: chen hao@zjweu.edu.cn

**Abstract:** Constructing a precise and effective evaluation index system is crucial to flood disaster prevention and management in coastal areas. This study takes Lucheng District, Wenzhou City, Zhejiang Province, southeastern China, as a case study and constructs an evaluation index system comprising three criterion levels: disaster-causing factors, disaster-gestation environments, and disaster-bearing bodies. The weights of each evaluation index are determined by combining the Analytic Hierarchy Process (AHP) and the entropy method. The fuzzy matter-element model is utilized to assess the flood disaster risk in Lucheng District quantitatively. By calculating the correlation degree of each evaluation index, the comprehensive index of flood disaster risk for each street area is obtained, and the flood disaster risk of each street area is classified according to the risk level classification criteria. Furthermore, the distribution of flood disaster risks in Lucheng District under different daily precipitation conditions is analyzed. The results indicate that: (1) the study area falls into the medium-risk category, with relatively low flood risks; (2) varying precipitation conditions will affect the flood resilience of each street in Lucheng District, Wenzhou City. The flood disaster evaluation index system and calculation framework constructed in this study provide significant guidance for flood risk assessment in coastal plain cities.

**Keywords:** coastal plain cities; flood disasters; risk assessment; index system; fuzzy matter-element model



**Citation:** Huang, S.; Xuan, W.; Qiu, H.; Ye, J.; Chen, X.; Nie, H.; Chen, H. Assessing Flood Risks in Coastal Plain Cities of Zhejiang Province, Southeastern China. *Water* **2024**, *16*, 3208. <https://doi.org/10.3390/w16223208>

Academic Editor: Francesco De Paola

Received: 4 October 2024

Revised: 7 November 2024

Accepted: 7 November 2024

Published: 8 November 2024



**Copyright:** © 2024 by the authors. Licensee MDPI, Basel, Switzerland. This article is an open access article distributed under the terms and conditions of the Creative Commons Attribution (CC BY) license (<https://creativecommons.org/licenses/by/4.0/>).

## 1. Introduction

With the change in climate and the increasing speed of urbanization, the recurrence and concentration of urban waterlogging disasters and misfortunes increase yearly [1–3]. Hence, urban waterlogging has become one of the most common catastrophes influencing the advancement and economy, and it has also been recognized by the world as the greatest challenge for sustainable water management in the 21st century [4,5].

Zhejiang Province is on the southeast coast of China, with a land area of 105,500 square kilometers. The landscape of this region slopes from southwest to northeast. The northeast and east coasts are mostly fields shaped by waterways and lake alluvial and shallow ocean stores. From north to south, it is divided into five plains: Hangjiahu, Xiaoshao, Ningbo, Taizhou, and Wenzhou Coastal. The five plains account for 15% of the province's land area, 50% of the province's population, and more than 70% of its businesses and occupy a significant position within the financial and social improvement of the area [6].

The reasons for waterlogging in cities and towns in the coastal plain and river network area are first that the geographical location is vulnerable to tropical storms and downpours;

the territory is low-lying, and the mountains face the ocean. The upper part of the mountains is overwhelmed, while the tide supports the lower part. Additionally, the drainage conditions are innately poor. Secondly, with the increasing speed of urbanization, the expansion of urban ranges, the solidifying of the basic surface, the occupation of water areas, and the construction of foundations, damage to the initial stream arrangement and water system occurs which changes the storage capacity of the coastal plain zone. Finally, due to the extraordinary climate, wind, storm, and tides are unpredictable. The probability of these elements combining increases, causing floods to return to the channel within the polder area or flood control encirclement. As the water level of the external waterway continues to rise, the drainage outlets expand into the ocean, resulting in a severe flood drainage situation in the coastal plain river network [7–11].

Urban waterlogging drainage relies primarily on self-draining using the tide in the coastal plain river network area and is augmented by forced drainage. The main issue is that the water level of the inland river and the tide level of the outer river severely limit the ability of the region to drain [12,13]. Inland river water is suitable for daily tidal drainage, but the time is limited. When heavy rainfall occurs, the consistently high level of inland rivers obstructs urban drainage, causing widespread flooding in the metropolis. Floods, waterlogging, and tides all impact flood disasters in coastal plain river network cities. The boundary hydrological conditions are complicated and unique, with distinct systems and processes that might cause disasters [14,15]. To increase the precision of disaster prediction, attention should be paid to developing an efficient and real-time flood forecasting mathematical model. Additionally, it is necessary to create and innovate drainage system risk management and assessment methods and formulate corresponding drainage scheduling decision-making systems to improve urban waterlogging emergency management and scheduling capabilities [16,17].

A flood loss evaluation model based on spatial analysis technology that integrates GIS technology, database technology, flood forecasting and numerical simulation, remote sensing analysis, asset evaluation, and prediction analysis is known as GIS-based flood loss analysis technology [18,19]. Integrating GIS spatial analytic technology into the earlier loss assessment method is key [20–22]. In contrast to traditional statistical assessment results, which have a weaker ability to reflect the spatial characteristics of data, GIS spatial analytic technology uses various types of spatial data as the primary data source, and the output results contain a large amount of spatial data information. As a result, it can better support disaster relief and disaster reduction plans [23–25].

The typical Zhejiang Province district, especially the Lucheng district in the Wenzhou coastal plain, was chosen as the case study. The primary objectives of this study are (1) to develop a comprehensive index system for evaluating flood disaster risk, particularly in the context of the unique hydrological conditions of the coastal plain river network, and (2) to apply and validate this index system using a case study in the Lucheng district of Wenzhou, Zhejiang Province, by integrating GIS technology with flood forecasting models, numerical simulations, and spatial analysis techniques. Through this integrated approach, we aim to enhance the accuracy of flood disaster risk assessment and provide valuable insights for improving urban waterlogging emergency management and scheduling capabilities. This paper is organized as follows: Section 2 introduces the study area and data; the basic methods, including the construction of the index system, the data processing technique, and the fuzzy matter-element model, are described in Section 3; Section 4 presents the findings and discussions; finally, the conclusions are described in Section 5.

## 2. Study Area and Data

### 2.1. Study Area

Lucheng District, located in the southeast of Zhejiang Province, is a district under the jurisdiction of Wenzhou City. It is the seat of the Wenzhou Municipal People's Government and serves as the political, economic, and cultural center of Wenzhou City. Figure 1 illustrates the location of the study area. The district boasts a developed economy and a

dense population of 1.209 million. It covers a total land area of 292.8 square kilometers, including 15,549.99 hectares of agricultural land, 8700.00 hectares of construction land, and 3850.10 hectares of water. For our study, we selected eight highly urbanized sub-district administrative units within Lucheng District, including Nanjiao, Puxie, Wuma, Binjiang, Guanghua, Danan, Nanhui, and Songtai (the area enclosed by the bold red wireframe in Figure 1). This district experiences subtropical ocean monsoons. The hottest month is July, with an average temperature of 27 °C, while January is the coldest with an average temperature of 7.6 °C. The annual average temperature is 18 °C. The annual precipitation ranges from 1100 to 2200 mm, and the frost-free period lasts roughly 280 days. The Lucheng district's terrain consists primarily of plains, mountains, hills, and islands. Typhoons, rainstorms, floods, droughts, hot temperatures, lightning strikes, and landslides are natural disasters that occasionally happen.

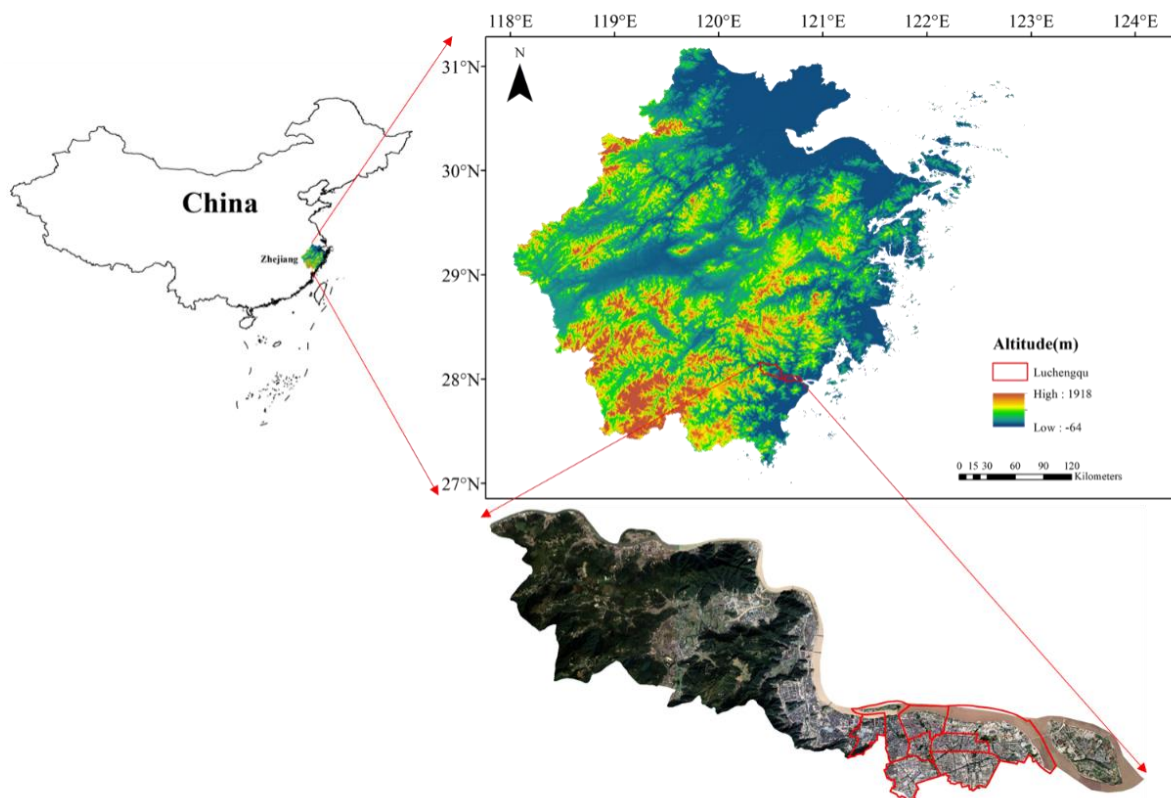


**Figure 1.** Location of the study area and the eight highly urbanized sub-districts.

## 2.2. Data

The main objective of urban flood disaster risk assessment is to use socio-economic data, such as population and property in the demonstration area, to calculate the flood risk and property and personnel losses based on the spatial and temporal distribution data obtained from rainfall-runoff and flood forecasting models, as well as using GIS platform. It provides a basis for decision-making regarding flood control and scheduling. The following is a list of the data that were used in the study:

Digital elevation model (DEM) data with a resolution of 30 m were downloaded from the Geospatial Data Cloud (<http://www.gscloud.cn> (accessed on 5 September 2024), the highest resolution available for the public); land cover data with a resolution of 1 km were downloaded from the Global Land Cover 2000 project (<https://globalmaps.github.io/glcnm.html> (accessed on 5 September 2024)); the daily data of meteorological/hydrological stations and the control operation data of various water conservancy facilities in the Lucheng district were obtained from the Wenzhou Bureau of Hydrology and Water Re-

sources; economic and social data were obtained from the Wenzhou Bureau of Statistics, including road traffic, administrative area, industrial area, and population distribution.

### 3. Methodology

The process of this study is outlined in Figure 2. Initially, a database is constructed to systematically collect topographic, hydrometeorological, and socio-economic data, providing a comprehensive and accurate information foundation for the assessment. Subsequently, the data are imported into an indexing system, encompassing both subjective and objective enabling indicators to reflect the diverse characteristics of disaster risks fully. On the ArcGIS platform, a consistency check is conducted to ensure the accuracy and uniformity of all data, laying a solid foundation for subsequent assessment tasks. Next, game theory methods are utilized to perform weight combinations for various indicators, scientifically determining their importance in risk assessment, thus making the assessment results more objective and reasonable. Then, a fuzzy matter-element model based on correlation degree is employed to deeply analyze the internal relationships among indicators, further enhancing the precision and reliability of the risk assessment. Finally, the risk assessment stage begins, where a comprehensive evaluation of flood disaster risks is conducted by analyzing multiple aspects such as historical flood characteristics, hazard factors, risk responses, and changes in the disaster management environment. This provides scientific evidence and decision-making support for disaster management and response.

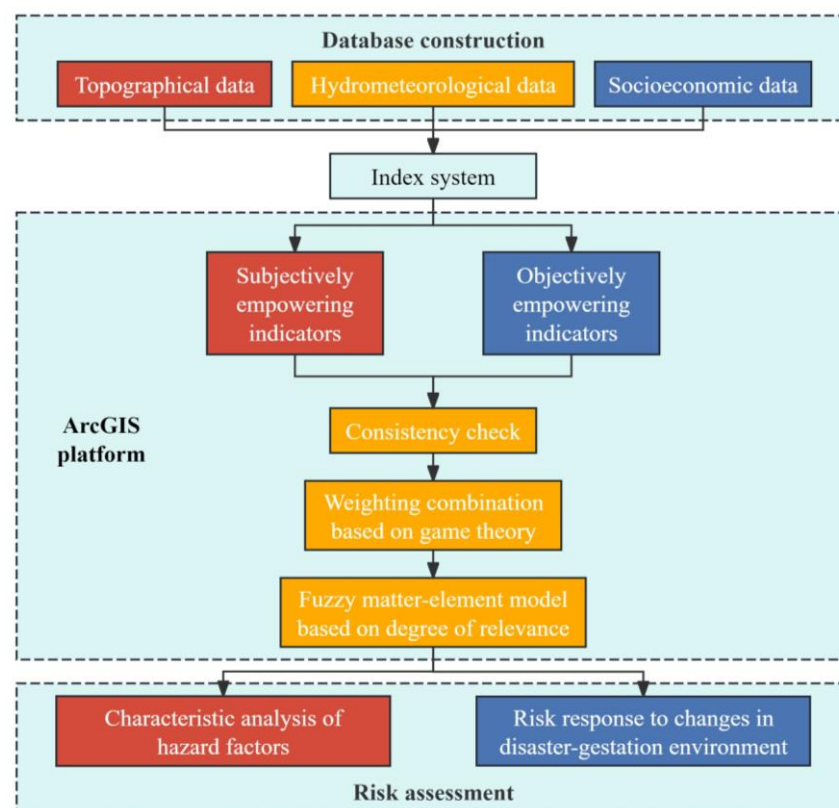


**Figure 2.** The general framework of the study.

#### 3.1. Flood Disaster Risk System

The regional flood disaster system consists of disaster-gestation settings, disaster-causing forces, and disaster-bearing bodies and is a system of abnormal changes on the earth's surface [26–29]. The hydrological, climatic, and underlying surface conditions are among the habitats that are disaster-prone. The degree of dynamic changes in the environment, or its stability or sensitivity, will impact the frequency and intensity of disasters. Instead of the atmospheric and hydrometeorological environments, the underlying surface

environment has a greater impact on the geographical distribution of flood disaster risk for small and local locations. The underlying surface environment, river networks, surface cover, and soil influence the likelihood of flooding. Therefore, to assess the stability of flood disaster-prone ecosystems, topography, river and lake distribution, land use, and vegetation coverage are chosen as evaluation indices. The bodies susceptible to disasters contain people and their activities, society, and resources. Varied disaster-bearing bodies frequently exhibit different vulnerability characteristics. Age, gender, and physical condition are three variables that directly determine how badly floods can hurt people. The capacity of buildings to withstand flood disasters is directly influenced by their material, construction, number of floors, and lifespan. The amount of annual precipitation, the anomaly of precipitation during the rainy season, the average maximum 3-day precipitation, the number of annual rainstorm days, and the peak discharge of the standard area are currently the main indicators for determining the extent of damage caused by flood disasters [30–33].

### 3.2. Assessment Index System

Construction of the flood disaster risk assessment index system is highly difficult due to the complexity of the flood disaster system, the unpredictability of the flood disaster risk, and the variety of flood disaster influencing elements [34–36]. The following guidelines should be followed in order to create a system for measuring flood disaster risk that is scientific, thorough, reasonable, and useful: (1) the index must be connected in some way to the risk, and this relationship may be quantitative or semi-quantitative, and it may reflect the risk's hazard, magnitude, and level directly or indirectly; (2) to quantify and visualize the fuzzy risks, the data are as spatial as possible and strive to reflect the spatial distribution pattern of regional flood disaster risks; (3) indexes should be acquired using global positioning, geographic information systems, and remote sensing technologies; (4) the index system should be functional and accurately reflect all of the information in the flood disaster system.

In flood disaster risk assessment, adopting a hierarchical structure is grounded in the intricate and multifaceted nature of flood disasters. This structural framework is meticulously designed to encapsulate the relationships among the various components of risk assessment, ensuring a comprehensive and systematic evaluation process. At the Target Level, the primary focus is quantifying and understanding the regional flood disaster risk. This level serves as the macro-perspective, assessing the size and severity of potential flood risks. It provides a holistic view, enabling decision-makers to grasp the broader implications of flood disasters on a regional scale. The Criterion Level is established based on the recognition that risk is a multifaceted concept, encompassing the likelihood of an event, its stability (or predictability), and the vulnerability of the affected area. These three factors—risk, stability, and vulnerability—form the cornerstone of our assessment criteria. By evaluating these dimensions, the complex interplay between risk factors and their potential impacts can be better understood. The Index Level refines the assessment into specific, measurable indicators. This level is highly flexible, allowing for the inclusion of multiple degrees of index layers tailored to the specific needs of the assessment. For instance, disaster-causing factors such as typhoons, tsunamis, dike breaches, and severe rainfall are crucial indicators of the potential for flood events. Similarly, the environment's vulnerability, including terrain, water systems, flora, and land type, significantly determines the severity and spread of floods. Additionally, population, housing, agriculture, and economic indexes reflect the potential socio-economic impacts of flood disasters, highlighting the disaster-prone entities within the region (Figure 3).

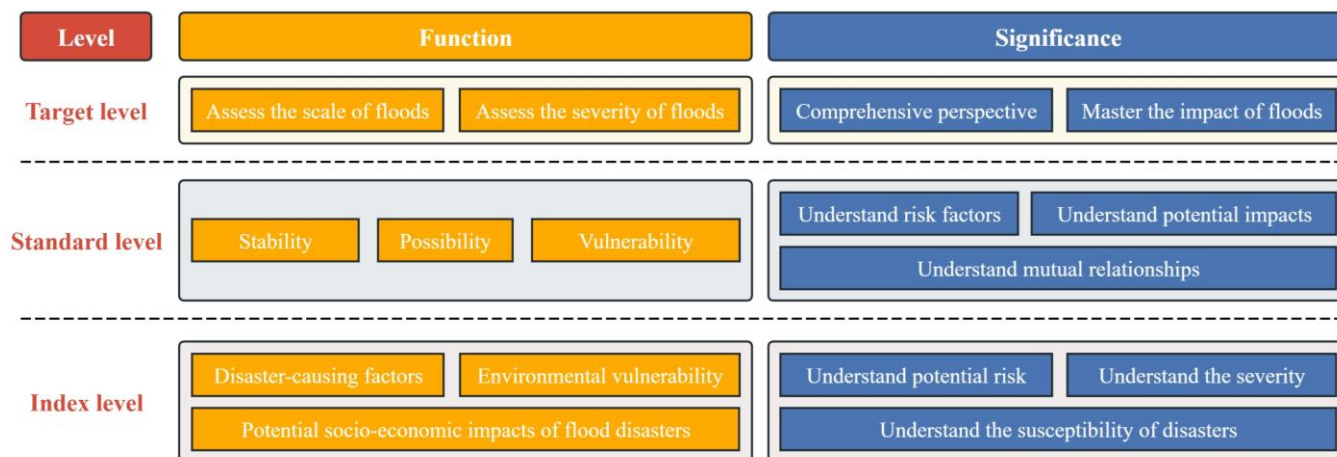


**Figure 3.** The layered structure of flood disaster assessment.

This hierarchical classification justifies its ability to provide a structured yet flexible flood disaster risk assessment framework. Decomposing the complex risk into manageable components facilitates a detailed and precise analysis of each factor’s contribution to the overall risk. Furthermore, this approach ensures that no crucial aspect is overlooked, enhancing the comprehensiveness and accuracy of the assessment. Ultimately, such a hierarchical structure supports evidence-based decision-making, enabling stakeholders to develop and implement effective flood disaster management strategies (Table 1).

**Table 1.** Flood disaster risk assessment index system in Lucheng district.

Target Level	Criterion Level	Index Level	Meaning	Attribute
Disaster-causing factors (A <sub>1</sub> )	Rainfall (B <sub>1</sub> )	Precipitation (C <sub>1</sub> )	The amount of water that falls to the ground within a certain period	Negative correlation
		Rainstorm duration (C <sub>2</sub> )	The duration of continuous or intermittent rainstorms	Negative correlation
		Sink flow (C <sub>3</sub> )	The amount of water that seeps into the soil through a unit area of soil layer per unit time	Positive correlation
Disaster-gestation environment (A <sub>2</sub> )	Vegetation (B <sub>2</sub> )	Vegetation cover (C <sub>4</sub> )	The degree to which plants cover the surface	Positive correlation
	Rivers (B <sub>3</sub> )	River network density (C <sub>5</sub> )	The number of total length of rivers per unit area	Negative correlation
	Topography (B <sub>4</sub> )	Elevation standard deviation (C <sub>6</sub> )	The degree of terrain undulation	Negative correlation
Disaster-bearing body (A <sub>3</sub> )	Population (B <sub>5</sub> )	Total population per unit area (C <sub>7</sub> )	Population density	Negative correlation
		Old and young population per unit area (C <sub>8</sub> )	The number of elderly and children per unit area	Negative correlation
		GDP output value per unit area (C <sub>9</sub> )	Economic density of the region	Negative correlation
	Housing (B <sub>6</sub> )	House value (C <sub>10</sub> )	The market price or assessed value of a house	Negative correlation
Agriculture (B <sub>7</sub> )	Type and area of crops (C <sub>11</sub> )	Types of crops planted and land area occupied	Determined by crop tolerance	

### 3.3. Combination of Weighting Methods

Index weights can be calculated using one of two basic approaches, namely subjective and objective weighting methods [37]. The primary subjective weighting methods are the Delphi method, binomial coefficient method, analytic hierarchy process, and chain ratio scoring method. It is a technique for allocating weights based on individuals' subjective relevance on each evaluation index [38]. The principal component analysis method, the average method, and the entropy approach are the key components of the objective weighting methods. The matching index weight is determined depending on the volume of the original data [39]. Each of these two different approaches has benefits and drawbacks [40,41]. Using the objective weighting method to determine the weight coefficient is more objective in most cases, but it is at odds with the actual importance of each index, making it challenging to explain the results clearly. The subjective weighting method has weak objectivity but strong interpretation. This paper adopted the analytic hierarchy process as the analysis method of the subjective weighting method. The entropy method was used as the analysis method of the objective weighting method.

By combining subjective and objective weighting methods, this study aims to balance the interpretability of subjective insights and the objectivity of data-driven analysis. Integrating the Analytic Hierarchy Process (AHP) and the entropy method allow for a dual validation of weights, where subjective assessments are cross-checked against objective data patterns. This hybrid approach enhances the credibility and transparency of the weighting process and ensures that the final weights are contextually meaningful and statistically sound. Furthermore, the complementarity between subjective and objective methods can address potential biases and limitations inherent in each method. Subjective methods can be corrected for any undue emphasis on variability that might be overstated by objective methods, especially in cases where certain indices, despite low variability, are critical for capturing the essence of the phenomenon under study. Conversely, objective methods can counteract potential over-reliance on subjective judgments, ensuring that the weights are grounded in the actual data characteristics and are not unduly influenced by individual biases or preferences.

The concept of the system analysis is embodied in the combination weighting approach, which integrates subjective and objective weighing data [42]. The combined weighting approach was used to establish the index weight because both the subjective and the objective weighing methods have benefits and drawbacks of their own. A combination of weighting methods can consider decision-makers preferences for attributes and reduce the subjective arbitrariness of weighting. Decision-making outcomes are more realistic and reliable when subjective and objective weighting of index attributes is achieved.

Before adopting the combined weighting method, we must first check the consistency of the weight results calculated by different weight calculation methods since the weight indexes calculated by different weights will be different and even in conflict. Suppose that the weights determined by  $k$  weight calculation methods are to be combined weighting. When  $k = 2$ , the consistency test of the subjective and objective weighting method uses the Spearman rank correlation coefficient to characterize. Distance function,  $d(W^{(1)}, W^{(2)}) = \left[ \frac{1}{2} \sum_{j=1}^n (w_j^{(1)} - w_j^{(2)})^2 \right]^{\frac{1}{2}}$ , can describe the degree of consistency of subjective and objective empowerment methods. When  $0 \leq d(W^{(1)}, W^{(2)}) \leq 1$ , the smaller  $d(W^{(1)}, W^{(2)})$ , the closer the result of subjective and objective empowerment [43].

Game theory analyzes rational behavior and decision balance when multiple decision-making subjects influence each other [44]. According to game theory, each strategy is the outcome of rational decision-making, wherein each player seeks to maximize their interests or minimize their losses. The decision-makers of all parties work together to reach the desired outcome, which is not under the power of any one party. By minimizing the difference between the total weight and each weight, Nash equilibrium seeks consistency

and compromise between various weights to reduce the total variances and maximize shared interests. The steps of weighting combination based on game theory are:

(1) For a basic weight set  $U = \{u_1, u_2, \dots, u_n\}$ ,  $n$  vectors are arbitrarily combined into a set of possible weights:

$$u^* = \sum_{k=1}^n \alpha_k^* u_k \quad (1)$$

where  $u$  is a possible weight vector of the set of possible weight vectors,  $\alpha_k$  is weight coefficient.

(2) The combination of weighting methods of game theory can find the most satisfactory  $u^*$  in possible vector sets. The basic idea is to minimize the deviations between the possible weights and the basic weights, that is, to find agreement or compromise between different weights. Therefore, finding the most satisfactory weight vector is equivalent to optimizing the linear combination coefficient  $\alpha_k$ , so that the dispersion between  $u$  and each  $u_k$  is minimized:

$$\min \left\| \sum_{j=1}^n \alpha_j \times u_j^T - u_i^T \right\|_2 \quad (i = 1, 2, \dots, n) \quad (2)$$

According to the differential properties of the matrix, it can be concluded that the optimal first derivative condition of the above formula is:

$$\sum_{j=1}^n \alpha_j \times u_j \times u_i^T = u_i \times u_i^T \quad (i = 1, 2, \dots, n) \quad (3)$$

(3) Due to the selected indicators' different data sources, units, and dimensions, to effectively reflect each indicator's impact on the risk of rainstorms and flood disasters, it is necessary to normalize the indicator data. During the normalization process, indicators are classified as positive and negative attributes. Positive indicators refer to those where a higher numerical value indicates a greater likelihood or impact of flood disasters; conversely, negative indicators refer to those where a higher numerical value indicates a lower likelihood or impact of flood disasters.

For positive indicators, the normalization formula is:

$$y = \frac{x - x_{\min}}{x_{\max} - x_{\min}} \quad (4)$$

For negative indicators, the normalization formula is:

$$y = \frac{x_{\max} - x}{x_{\max} - x_{\min}} \quad (5)$$

where  $x$  and  $y$  represent the original and normalized values of the indicator, respectively, and  $x_{\min}$  and  $x_{\max}$  represent the minimum and maximum values of the indicator, respectively.

Get  $(\alpha_1, \alpha_2, \dots, \alpha_n)$ , normalize, and finally get the combined weight as:

$$u^* = \sum_{k=1}^n \alpha_k^* u_k \quad (6)$$

Firstly, the comparison of the judgment matrix of the analytic hierarchy process is obtained, as shown in Table 2. Afterwards, the weights of the flood risk assessment index system in Lucheng District were calculated using the Analytic Hierarchy Process (Table 3) and Entropy Method (Table 4) respectively.



**Table 2.** Judgment matrix and determined weights in the analytic hierarchy process.

Judgment Index		Eigenvector	Consistency Check
A <sub>1</sub> B <sub>1</sub>	B <sub>1</sub> 1	1	
A <sub>2</sub> B <sub>2</sub> B <sub>3</sub> B <sub>4</sub>	B <sub>2</sub> 1 3 3	B <sub>3</sub> 1/3 1 1	B <sub>4</sub> 1/3 1 1
		0.1800 0.4100 0.4100	$\lambda_{\max} = 3.0503$ C.R. = 0.043
A <sub>3</sub> B <sub>5</sub> B <sub>6</sub> B <sub>7</sub>	B <sub>5</sub> 1 3 5	B <sub>6</sub> 1/3 1 1	B <sub>7</sub> 1/5 1 1
		0.1140 0.4054 0.4806	$\lambda_{\max} = 3.029$ C.R. = 0.028
B <sub>1</sub> C <sub>1</sub> C <sub>2</sub> C <sub>3</sub>	C <sub>1</sub> 1 3 3	C <sub>2</sub> 1/3 1 1	C <sub>3</sub> 1/3 1 1
		0.1800 0.4100 0.4100	$\lambda_{\max} = 3.0503$ C.R. = 0.043
B <sub>2</sub> C <sub>4</sub>	C <sub>4</sub> 1		1
B <sub>3</sub> C <sub>5</sub>	C <sub>5</sub> 1		1
B <sub>4</sub> C <sub>6</sub>	C <sub>6</sub> 1		1
B <sub>5</sub> C <sub>6</sub> C <sub>7</sub> C <sub>8</sub>	C <sub>6</sub> 1 3 5	C <sub>7</sub> 1/3 1 1	C <sub>8</sub> 1/5 1 1
		0.1140 0.4054 0.4806	$\lambda_{\max} = 3.029$ C.R. = 0.028
B <sub>6</sub> C <sub>10</sub>	C <sub>10</sub> 1		1
B <sub>7</sub> C <sub>11</sub>	C <sub>11</sub> 1		1

**Table 3.** Weight values of the flood disaster risk assessment index system in Lucheng district (Analytic Hierarchy Process).

Target Level	Criterion Level	Index Level
Disaster-causing factors (A <sub>1</sub> )	Rainfall (B <sub>1</sub> = 1)	Precipitation (C <sub>1</sub> = 0.1800) Rainstorm duration (C <sub>2</sub> = 0.4100) Sink flow (C <sub>3</sub> = 0.4100)
Disaster-gestation environment (A <sub>2</sub> )	Vegetation (B <sub>2</sub> = 0.1800) Rivers (B <sub>3</sub> = 0.4100) Topography (B <sub>4</sub> = 0.4100)	Vegetation cover (C <sub>4</sub> = 1) River network density (C <sub>5</sub> = 1) Elevation standard deviation (C <sub>6</sub> = 1)
Disaster-bearing body (A <sub>3</sub> )	Population (B <sub>5</sub> = 0.1140) Housing (B <sub>6</sub> = 0.4054) Agriculture (B <sub>7</sub> = 0.4806)	Total population per unit area (C <sub>7</sub> = 0.1140) Old and young population per unit area (C <sub>8</sub> = 0.4054) GDP output value per unit area (C <sub>9</sub> = 0.4806) House value (C <sub>10</sub> = 1) Type and area of crops (C <sub>11</sub> = 1)

After calculation, the weight of  $d(w^{(1)}, w^{(2)})$  calculated by the two methods is 0.38, which is between 0 and 1, meets the standard of the consistency of the test method, indicating that the weights obtained by the two weighting methods in this study are consistent. MATLAB (version R2023a) was adopted to execute the weighting combination method using the game theory, and the results are shown in Table 5. The flood disaster risk assessment results are expressed in the form of risk level and risk index. Risk levels can generally

be divided into 3 levels, 5 levels, and 10 levels. This paper uses five levels: highest-risk area, higher-risk area, medium-risk area, lower-risk area, and lowest-risk area (Table 6).

**Table 4.** Weight values of the flood disaster risk assessment index system in Lucheng district (Entropy Method).

Target Level	Criterion Level	Index Level
Disaster-causing factors (A <sub>1</sub> )	Rainfall (B <sub>1</sub> = 1)	Precipitation (C <sub>1</sub> = 0.1753) Rainstorm duration (C <sub>2</sub> = 0.2206) Sink flow (C <sub>3</sub> = 0.4497)
Disaster-gestation environment (A <sub>2</sub> )	Vegetation (B <sub>2</sub> = 0.384) Rivers (B <sub>3</sub> = 0.508) Topography (B <sub>4</sub> = 0.108)	Vegetation cover (C <sub>4</sub> = 1) River network density (C <sub>5</sub> = 1) Elevation standard deviation (C <sub>6</sub> = 1)
Disaster-bearing body (A <sub>3</sub> )	Population (B <sub>5</sub> = 0.4497) Housing (B <sub>6</sub> = 0.2206) Agriculture (B <sub>7</sub> = 0.3297)	Total population per unit area (C <sub>7</sub> = 0.327) Old and young population per unit area (C <sub>8</sub> = 0.405) GDP output value per unit area (C <sub>9</sub> = 0.268) House value (C <sub>10</sub> = 1) Type and area of crops (C <sub>11</sub> = 1)

**Table 5.** Calculated weights using the weighting combination method.

Unit System		w <sup>(1)</sup>	w <sup>(2)</sup>	w
A <sub>1</sub>	B <sub>1</sub>	1	1	1
A <sub>2</sub>	B <sub>2</sub>	0.1800	0.384	0.282
	B <sub>3</sub>	0.4100	0.508	0.459
	B <sub>4</sub>	0.4100	0.108	0.259
A <sub>3</sub>	B <sub>5</sub>	0.1140	0.4497	0.292
	B <sub>6</sub>	0.4054	0.2206	0.303
	B <sub>7</sub>	0.4806	0.3297	0.405
B <sub>1</sub>	C <sub>1</sub>	0.1800	0.1753	0.178
	C <sub>2</sub>	0.4100	0.2206	0.325
	C <sub>3</sub>	0.4100	0.4497	0.427
B <sub>2</sub>	C <sub>4</sub>	1	1	1
B <sub>3</sub>	C <sub>5</sub>	1	1	1
B <sub>4</sub>	C <sub>6</sub>	1	1	1
B <sub>5</sub>	C <sub>7</sub>	0.1140	0.327	0.231
	C <sub>8</sub>	0.4054	0.405	0.405
	C <sub>9</sub>	0.4806	0.268	0.364
B <sub>6</sub>	C <sub>10</sub>	1	1	1
B <sub>7</sub>	C <sub>11</sub>	1	1	1

**Table 6.** Classification of flood disaster risk.

Comment Rating	Lowest-Risk	Lower-Risk	Medium-Risk	Higher-Risk	Highest-Risk
Composite index	0.90~1.0	0.75~0.90	0.5~0.75	0.25~0.5	0~0.25

### 3.4. Fuzzy Matter-Element Model Based on Degree of Relevance

#### 3.4.1. Hierarchy Extension of Matter-Element Method

Given the name of a factor N, the value of this name concerning feature c is v. Matter element refers to the use of ordered triples R = (N, c, v) as the basic element to describe factors [45–49]. According to the definition of matter element, v is determined by N

and  $c$ , denoted as  $v = c(N)$ . Therefore, the matter element can also be expressed as  $R = (N, c, c(N))$ .

A factor has multiple characteristics, if the factor  $n$  characteristics describe  $N$   $c_1, c_2, \dots, c_n$  and its corresponding values are  $v_1, v_2, \dots, v_n$ , it can be expressed as:

$$R = \begin{bmatrix} N, & c_1, & v_1 \\ N, & c_2, & v_2 \\ \vdots & \vdots & \vdots \\ N & c_n & v_n \end{bmatrix} = (N, C, V) \tag{7}$$

Call  $R$  the  $n$ -dimensional matter element, in which:

$$C = \begin{bmatrix} c_1 \\ c_2 \\ \vdots \\ c_n \end{bmatrix}, V = \begin{bmatrix} v_1 \\ v_2 \\ \vdots \\ v_n \end{bmatrix} \tag{8}$$

The matter-element model with the extension set theory is organically combined with the matter-element extension set. The matter element is a perfect carrier that carries quantitative and qualitative information. According to the matter-element model and extension of the set theory, the specific evaluation steps are as follows:

(1) To determine the classic domain

$$R_{0j} = (N_{0j}, C, x_{0ji}) = \begin{bmatrix} N_{0j} & c_1 & x_{0j1} \\ N_{0j} & c_2 & x_{0j2} \\ \vdots & \vdots & \vdots \\ N_{0j} & c_n & x_{0jn} \end{bmatrix} = \begin{bmatrix} N_{0j} & c_1 & \langle a_{0j1}, b_{0j1} \rangle \\ N_{0j} & c_2 & \langle a_{0j2}, b_{0j2} \rangle \\ \vdots & \vdots & \vdots \\ N_{0j} & c_n & \langle a_{0jn}, b_{0jn} \rangle \end{bmatrix} \tag{9}$$

where  $N_{0j}$  is the  $j$ -th security level of the evaluation object  $N$ ,  $j = 1, 2, \dots, h$ ;  $c_i$  is the  $i$ -th evaluation index,  $i = 1, 2, \dots, m$ ;  $x_{0ji}$  does the security level specify the value range  $N_{0j}$  concerning the index  $c_i$ , that is, the data range (classical domain) of each evaluation index  $c_i$  concerning each level  $N_{0j}$ . The classic domain of all security levels can be expressed as a matrix:

$$R_0 = \begin{bmatrix} N_0 & N_{01} & N_{02} & \dots & N_{0h} \\ c_1 & \langle a_{011}, b_{011} \rangle & \langle a_{021}, b_{021} \rangle & \dots & \langle a_{0h1}, b_{0h1} \rangle \\ c_2 & \langle a_{012}, b_{012} \rangle & \langle a_{022}, b_{022} \rangle & \dots & \langle a_{0h2}, b_{0h2} \rangle \\ \vdots & \vdots & \vdots & \dots & \vdots \\ c_m & \langle a_{01m}, b_{01m} \rangle & \langle a_{02m}, b_{02m} \rangle & \dots & \langle a_{0hm}, b_{0hm} \rangle \end{bmatrix} \tag{10}$$

(2) To determine the section domain

$$R_P = (P, C, x_P) = \begin{bmatrix} P & c_1 & x_{P1} \\ P & c_2 & x_{P2} \\ \vdots & \vdots & \vdots \\ P & c_n & x_{Pn} \end{bmatrix} = \begin{bmatrix} P & c_1 & \langle a_{0P1}, b_{0P2} \rangle \\ P & c_2 & \langle a_{0P2}, b_{0P2} \rangle \\ \vdots & \vdots & \vdots \\ P & c_n & \langle a_{0Pn}, b_{0Pn} \rangle \end{bmatrix} \tag{11}$$

where  $P$  is the entire security level, and  $x_{Pi} = \langle a_{0Pi}, b_{0Pi} \rangle$  is the range of the value specified by  $P$  on the index  $c_i$ , that is, the data range (section domain) obtained by the index  $c_i$  for all the security levels, obviously  $x_{0ji} \subset x_{Pi}$ .

(3) To evaluate the determined matter, the data or analysis results related to the evaluation object are expressed as:

$$R = \begin{bmatrix} P & c_1 & x_1 \\ P & c_2 & x_2 \\ \vdots & \vdots & \vdots \\ P & c_m & x_m \end{bmatrix} \tag{12}$$

where P is the object to be evaluated, and  $x_i$  is the value of the object P to be evaluated concerning the index  $c_i$ .

(4) To evaluate the degree of relevance of each index of the object concerning each level in extended mathematics, a set A in the universe  $U (-\infty, +\infty)$  is used to describe the degree to which the element u in U belongs to and does not belong to A. This degree is represented by  $K(u)$ ,  $-\infty < K(u) < +\infty$ . The function  $K(u)$  is the relevance function of U on the set A, and the function value of the relevance function is called the relevance. The degree of relevance is calculated using the following formula:

$$K_j(x_i) = \begin{cases} \frac{\rho(x_i, x_{0ji})}{\rho(x_i, x_{Pi}) - \rho(x_i, x_{0ji})}, & \rho(x_i, x_{Pi}) - \rho(x_i, x_{0ji}) \neq 0 \\ -\rho(x_i, x_{0ji}) - 1, & \rho(x_i, x_{Pi}) - \rho(x_i, x_{0ji}) = 0 \end{cases} \tag{13}$$

$$\rho(x_i, x_{0ji}) = \left| x_i - \frac{1}{2}(a_{0ji} + b_{0ji}) \right| - \frac{1}{2}(b_{0ji} - a_{0ji}) \tag{14}$$

$$\rho(x_i, x_{Pi}) = \left| x_i - \frac{1}{2}(a_{Pi} + b_{Pi}) \right| - \frac{1}{2}(b_{Pi} - a_{Pi}) \tag{15}$$

where  $\rho(x_i, x_{0ji})$  and  $\rho(x_i, x_{Pi})$ , respectively, represent the distance between the point and the interval,  $\rho(x_i, x_{0ji})$  represents the distance between point  $x_i$  and interval  $x_{0ji}$ , and  $\rho(x_i, x_{Pi})$  represents the distance between point  $x_i$  and interval  $x_{Pi}$ .

If the weight coefficient of the index  $c_i$  is  $\lambda_i$ , and  $\sum_{i=1}^n \lambda_i = 1$ , then  $K_j(P) = \sum_{i=1}^n \lambda_i K_j(x_i)$ .  $K_j(P)$  is the degree of relevance of each index of the object to be evaluated concerning each level, and the combined value in the case of considering the importance of the index, indicating the degree to which the object  $p_0$  to be evaluated belong to the set  $P_0$ .

(5) To rate the category, the degree of association  $K_j(P)$  has a certain physical meaning. When it is greater than 0, the evaluated object fully meets the level j; when it is less than -1, it does not belong to the level j. When it is between -1 and 0, it indicates that the evaluated object meets the level j, and the degree of compliance depends on the specific value of the degree of relevance. It is divided according to the optimal principle if it meets multiple levels.

If  $K_{j0}(P) = \max_{j \in \{1, 2, \dots, m\}} K_j(P)$ , then  $p_0$  belongs to rank  $j_0$ . Make  $\overline{K_j(P)} = \frac{K_j(P) - \min K_j(P)}{\max K_j(P) - \min K_j(P)}$ ,  $j^* = \frac{\sum_{j=1}^m j \overline{K_j(P)}}{\sum_{j=1}^m \overline{K_j(P)}}$ . Call  $j^*$  the characteristic value of the level variable of  $p_0$ . From the value of  $j^*$ , it can be judged that the degree to which the object to be assessed is biased toward the adjacent category.

### 3.4.2. Improvement of Single-Level Fuzzy Optimal Evaluation Model

The theoretical underpinnings of fuzzy optimization include fuzzy set theory and relative membership theory [50–54]. Multi-objective decision-making issues are frequently solved using fuzzy optimization. The target relative superiority degree and the decision relative superiority degree are two categories under which the relative membership degree can be subdivided in the optimization. The relative membership of the target to the superior is abbreviated as the target’s relative superiority degree, and the relative superiority of decision-making is abbreviated as the decision-relative making’s membership to the superior.

In multi-objective decision-making, the fuzzy optimization theory is frequently utilized, but a full judgment of the evaluation object is typically required in real-world situations. Therefore, comprehensive category differentiation is more important than ranking alone [55–58]. According to this theory, the membership degree calculation in the fuzzy optimization model is improved to achieve the purpose of ranking and optimization and reflect the grade level of the evaluation object through the superiority degree.

The relative superiority utility function is created by employing fuzzy theory to quantify and synthesize each target. Its value not only reflects the relative benefits and drawbacks of the scheme but also the worth and difficulty of the scheme, making it feasible to carry out grade evaluation using the fuzzy optimization theory. Because of the constrained decision-making framework of the fuzzy optimal decision-making issue, the maximum and minimum values of the indexes calculated by the maximum and minimum operators typically do not represent the ideal degree of the indexes. Therefore, the relative degree of membership obtained through this standardization method can only reflect a single index’s relative strengths and weaknesses in a scheme. The model needs to be updated to give the degree of superiority a specific objective value reflecting the program’s level.

The fundamental idea behind relative membership degree is to seek out the mapping relationship on the continuum by designating 1 and 0 to the maximum and minimum values of the scheme sample indexes as the poles of the reference system. The maximum and minimum values of the reference continuum are gradually approaching the continuum, which indicates that the relative membership degree is gradually approaching the absolute membership degree. This is the relationship between the relative and absolute membership degrees. The membership degree in the fuzzy optimization theory can be enhanced and optimized to give the index relative membership degree and the scheme superiority degree an “absolute” meaning, allowing fuzzy optimization to be applied to the evaluation of scheme levels. Using analogy and expert advice, the left and right basis points are created, and they are utilized in place of the minimum and maximum operators to calculate the degree of membership. The “unallowable value” of the evaluation index corresponds to the value of the left base point, and the “ideal value” corresponds to the value of the right base point. In the relative sense, the membership degree derived from this might be called the “absolute membership degree.”

Let  $x_i^{(a)}$  and  $x_i^{(b)}$  be the left and right base point values of the index set  $P_i$ , where  $x_i^{(a)} < x_i^{(b)}$ , the improved membership degree calculation formula is as follows:

(1) When the benefit index  $i \in O_1$

$$r_{ij} = \begin{cases} 1 & x_{ij} \geq x_i^{(b)} \\ \frac{x_{ij} - x_i^{(a)}}{x_i^{(b)} - x_i^{(a)}} & x_i^{(a)} < x_{ij} < x_i^{(b)} \\ 0 & x_{ij} \leq x_i^{(a)} \end{cases} \tag{16}$$

(2) When the cost index  $i \in O_2$

$$r_{ij} = \begin{cases} 0 & x_{ij} \geq x_i^{(b)} \\ \frac{x_i^{(b)} - x_{ij}}{x_i^{(b)} - x_i^{(a)}} & x_i^{(a)} < x_{ij} < x_i^{(b)} \\ 1 & x_{ij} \leq x_i^{(a)} \end{cases} \tag{17}$$

(3) When the middle index  $i \in O_3$

$$r_{ij} = \begin{cases} \frac{x_{ij} - x_i^{(a)}}{x_i^{(*)} - x_i^{(a)}} & x_i^{(a)} < x_{ij} \leq x_i^{(*)} \\ \frac{x_{ij} - x_i^{(a)}}{x_i^{(*)} - x_i^{(a)}} & x_i^{(*)} < x_{ij} < x_i^{(b)} \\ 0 & x_i^{(a)} \text{ or } x_{ij} \geq x_i^{(*)} \end{cases} \tag{18}$$

According to the above formula, the transformed node domain is  $\langle 0, 1 \rangle$ , and the classical domain is a single interval within  $\langle 0, 1 \rangle$ . This conversion idea is similar to the index membership degree calculation method. The node domain breakpoint value and the central optimal value as the conversion standard are equivalent to the base point value in the membership degree calculation.

#### 4. Results and Discussion

##### 4.1. Calculation of Disaster-Causing Factors

The eigenvalues of flood disaster risk assessment indexes in the Lucheng district were obtained, and the eigenvalues of each index were standardized using the vector normalization method. The flood disaster risk was divided into 5 levels, from highest to lowest, and standardized processing was performed according to the attributes of each index. Similarly, the threshold value of each index level is standardized according to the vector normalization method. The results of the standardization process are shown in Table 7. The range of values for each level, namely the classic domain and the section domain, are shown in Table 8.

**Table 7.** Grade standardization results of evaluation indexes.

Criterion Layer	Index Layer	Actual Value of Index (2017)	Index Evaluation Value	Forward/Inverse
Rainfall (B <sub>1</sub> )	Precipitation (C <sub>1</sub> )	0.35	0.87	-
	Rainstorm duration (C <sub>2</sub> )	0.66	0.58	-
	Infiltration rate (C <sub>3</sub> )	0.58	0.7	+

**Table 8.** Classical domain and sectional domain of evaluation index.

Evaluation Index	N <sub>01</sub>	N <sub>02</sub>	N <sub>03</sub>	N <sub>04</sub>	N <sub>05</sub>
Precipitation (C <sub>1</sub> )	$\langle 0.8, 1 \rangle$	$\langle 0.5, 0.8 \rangle$	$\langle 0.2, 0.5 \rangle$	$\langle 0.05, 0.2 \rangle$	$\langle 0, 0.05 \rangle$
Rainstorm duration (C <sub>2</sub> )	$\langle 0.7, 1 \rangle$	$\langle 0.55, 0.7 \rangle$	$\langle 0.35, 0.55 \rangle$	$\langle 0.2, 0.35 \rangle$	$\langle 0, 0.2 \rangle$
Infiltration rate (C <sub>3</sub> )	$\langle 0.7, 1 \rangle$	$\langle 0.5, 0.7 \rangle$	$\langle 0.4, 0.5 \rangle$	$\langle 0.25, 0.4 \rangle$	$\langle 0, 0.25 \rangle$

The first-level lower bound and the fifth-level upper bound are used, respectively, as the base point values for the evaluation levels according to the standards of the five evaluation levels divided by the table, and the membership degree matrix is calculated using the membership degree calculation method (Table 9).

**Table 9.** Basepoint value and subordination degree of flood disaster risk evaluation index in Lucheng district.

Criterion Layer	Index Layer	Left Base Point	Right Base Point	Subordination Degree	Weighted Value
Rainfall (B <sub>1</sub> )	Precipitation (C <sub>1</sub> )	0.05	0.8	0.9653	0.2620
	Rainstorm duration (C <sub>2</sub> )	0.2	0.7	0.7850	
	Infiltration rate (C <sub>3</sub> )	0.25	0.7	0.8431	

##### 4.2. Calculation of Disaster-Gestation Environments and Disaster-Bearing Bodies

In this study, we first delineated the extent of vegetation cover and utilized Digital Elevation Model (DEM) data to assess terrain variability by calculating the elevation standard deviation for each street. Subsequently, a hydrological analysis was conducted on the study area to map the distribution of the river network. Further, we calculated the density of the river network based on the river length and watershed area within each street’s watershed. Additionally, information such as total population per unit area, proportion of young and elderly populations, GDP output, housing prices, crop types, and disaster-affected areas

was directly obtained from yearbook data. To ensure data comparability and accuracy, these data were normalized. Next, we employed the Grey Relational Analysis method (Table 10) to conduct correlation analysis on various indicators and performed weighted calculations using weights determined by the combination weighting method. Ultimately, we derived the scores for each indicator and the comprehensive evaluation results (Table 11).

**Table 10.** Relevance calculation.

	Vegetation Cover	River Network Density	Elevation Standard Deviation	Total Population per Unit Area	Old and Young Population per Unit Area	GDP per Unit Area	House Value	Type and Area of Crops
Nanjiao	0.3766	0.6740	0.3596	0.3620	1.0000	0.7698	0.7333	0.3333
Puxieshi	0.3598	0.6636	0.3702	1.0000	0.3619	0.6143	0.7720	0.3333
Wuma	0.4044	0.3836	0.4530	0.9066	0.3636	1.0000	0.8020	0.3333
Binjiang	0.5036	0.6584	0.4057	0.4537	0.4159	0.3820	0.6235	0.3333
Guanghua	1.0000	0.5571	1.0000	0.4635	0.4159	0.3820	0.6235	0.3333
Danan	0.4721	1.0000	0.3830	0.7897	0.3668	0.7919	0.7173	0.3333
Nanhui	0.3627	0.5838	0.3742	0.4574	0.4137	0.4787	1.0000	0.3333
Songtai	0.5061	0.6261	0.4062	0.3935	0.5087	0.3762	0.9963	0.3333

**Table 11.** Score of each index factor and total evaluation.

Regional Index Factor	Disaster-Causing Factors (1/3)	Disaster-Pregnant Environments (1/3)			Disaster-Bearing Bodies (1/3)				Overall Evaluation	
	Vegetation Cover	River Network Density	Elevation Standard Deviation	Total Population per Unit Area	Old and Young Population per Unit Area	GDP per Unit Area	House Value	Type and Area of Crops		
Nanjiao	0.2620	0.1062	0.3094	0.0931	0.0244	0.1183	0.0818	0.2222	0.1350	0.626
Puxieshi	0.2620	0.1015	0.3046	0.0959	0.0675	0.0428	0.0653	0.2339	0.1350	0.611
Wuma	0.2620	0.1141	0.1761	0.1173	0.0612	0.0430	0.1063	0.2430	0.1350	0.594
Binjiang	0.2620	0.1420	0.3022	0.1051	0.0306	0.0492	0.0406	0.1889	0.1350	0.594
Guanghua	0.2620	0.2820	0.2557	0.2590	0.0313	0.0492	0.0406	0.1889	0.1350	0.676
Danan	0.2620	0.1331	0.4590	0.0992	0.0533	0.0434	0.0842	0.2173	0.1350	0.670
Nanhui	0.2620	0.1023	0.2679	0.0969	0.0308	0.0489	0.0509	0.3030	0.1350	0.608
Songtai	0.2620	0.1427	0.2874	0.1052	0.0265	0.0602	0.0400	0.3019	0.1350	0.628

According to the classification of the comprehensive index in Table 6, corresponding to the data in Table 11, under the design rainfall conditions, the comprehensive index of flood disasters of each street in the Lucheng district varies in size, and there is a slight difference. However, each street’s comprehensive index of flood disaster varies between 0.5 and 0.75. All of them are in the medium-risk zone. The exponential distribution is shown in Figures 4 and 5.

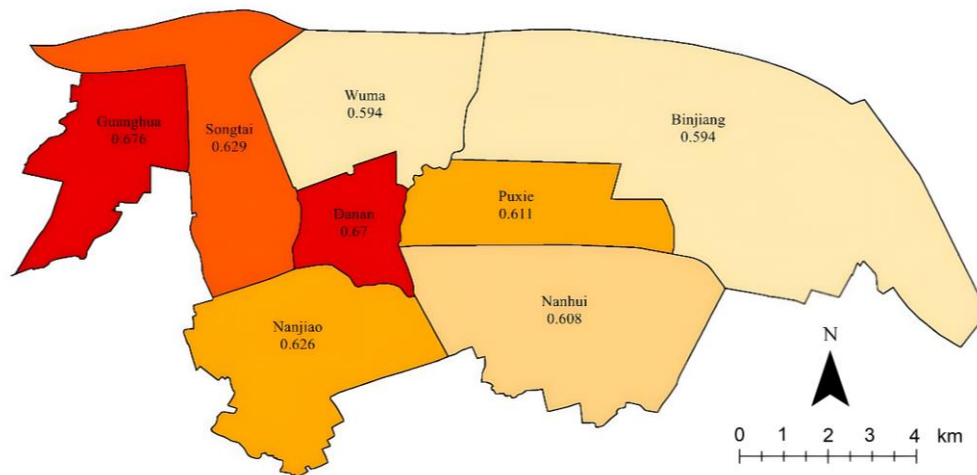


Figure 4. Geographical distribution map of flood risk assessment in Lucheng district.

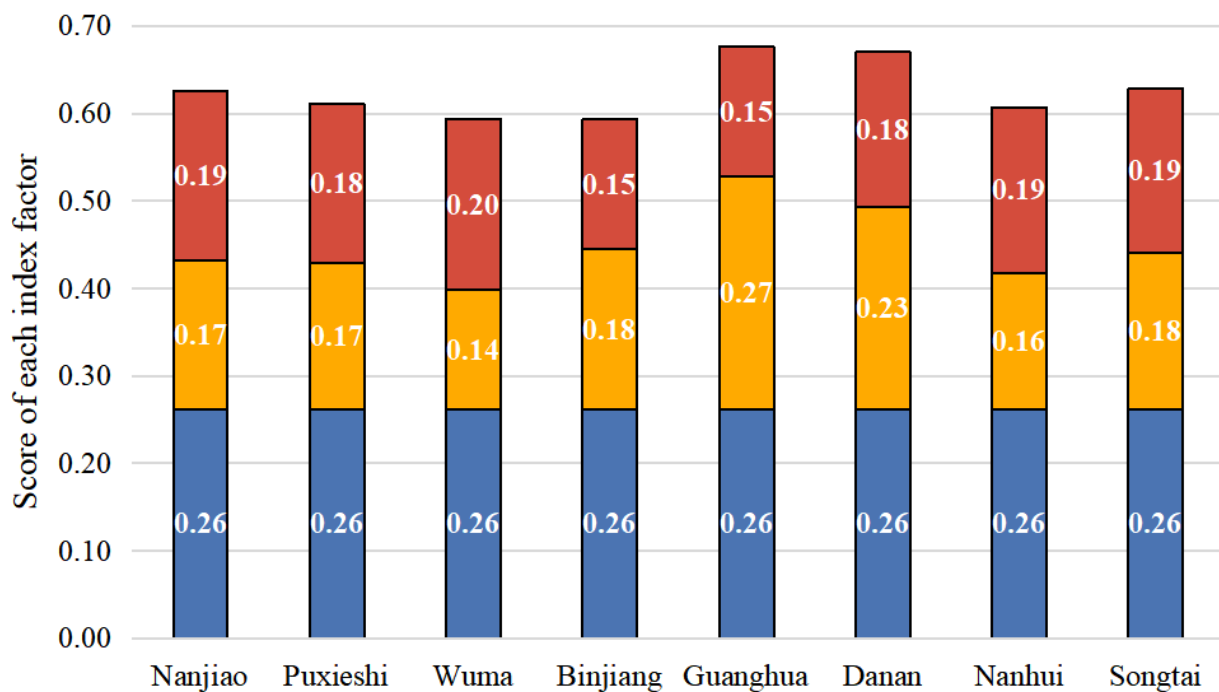


Figure 5. Comprehensive score distribution map of street area.

According to the data analysis results, the quantitative values for disaster-causing factors across all regions are 0.262, indicating that these regions have identical rainfall conditions in assessing disaster-causing factors. Regarding disaster-gestation environments, the Guanghua region has the highest quantitative value of 0.2656, while the Wuma region has the lowest value of 0.1358, demonstrating significant differences in disaster-gestation environments among different regions. Regarding disaster-bearing bodies, the Wuma region has the highest quantitative value of 0.1962, and the Binjiang region has the lowest value of 0.1481, indicating that there are also certain differences among regions in assessing disaster-bearing bodies.

The hazard factors (long rainfall and heavy rain) contribute to most of the total flood risk and are the main causes of urban flood disasters. The disaster-bearing body comes in second after the disaster-gestation conditions when there is little variation in rainfall across the different areas of the Lucheng district. The limit of the difference in the disaster-gestation environment score is 0.13, and the mean square error is 0.0018. The score of



difference limit of the disaster-bearing bodies is 0.5, and the mean square error is 0.0004. In contrast, there are significant differences between streets in the disaster-prone locations.

Figure 6 displays the secondary index score of the disaster-causing environment. By analyzing the trend of three secondary indexes, the river network density evaluation has the highest positive association with the evaluation of disaster-prone areas, except Guanghua Street. In disaster-prone areas, river network density is the most significant secondary index compatible with factor weighting. The ability to mitigate danger is generally higher in the denser the river network. Therefore, the total deployment should concentrate on regions with comparatively low river network density under severe weather conditions.

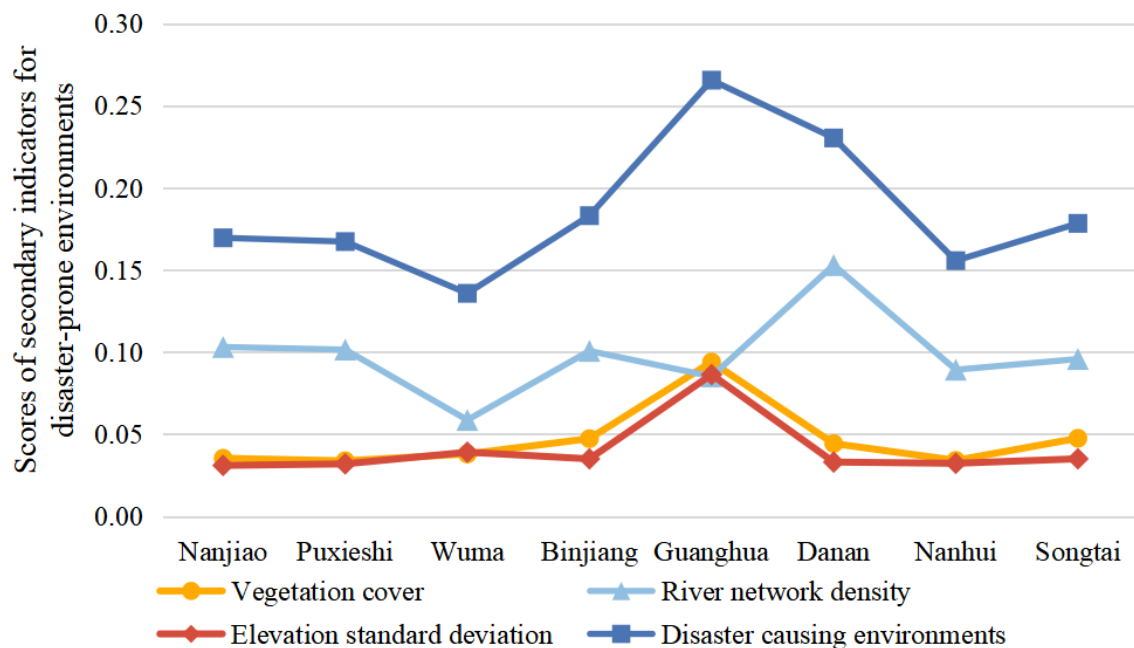


**Figure 6.** Line chart of secondary index scores of disaster-causing environments.

The regional change trends of the elevation standard deviation and vegetation coverage in each region are essentially parallel, demonstrating the strong correlation between the two indices. Moreover, Guanghua Street is distinctive in these regions. The terrain is steep, and there is good vegetation cover because the region is within the city's upper reaches. Although the river network has a low density, the combined effect of the two makes up for it, causing Guanghua Street to score highly and have a superior risk assessment than other regions. On the contrary, the probability of flooding is unpredictable in some dense river networks and downstream locations. In summary, low-lying areas downstream and areas with sparse river network density comprise most of the flood-risk areas in the Lucheng district.

#### 4.3. Calculation of Risk Assessment Based on Precipitation

According to applicable criteria, the Lucheng district experiences rainstorms when the average daily precipitation exceeds 50 mm. This computation is intended to set the daily precipitation as 50 mm, 150 mm, 250 mm, 350 mm, and 403.8 mm, respectively, in five scenarios, considering the local historical maximum 24 h precipitation of 403.8 mm. The comprehensive flood disaster index for the relevant street is calculated and analyzed using ArcGIS (version 10.8). Analysis chart, as shown in Figure 7.

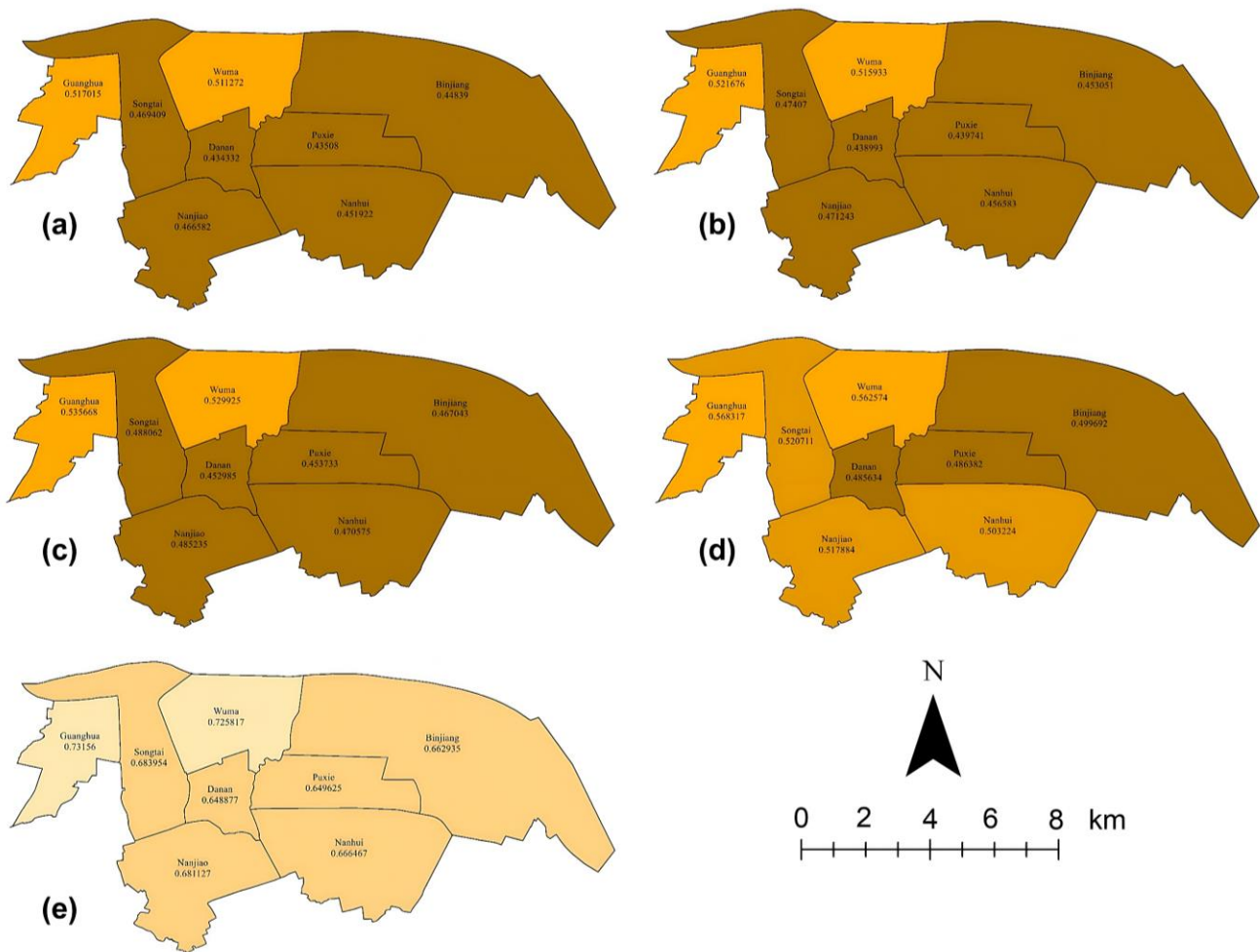


**Figure 7.** Distribution map of flood risk assessment in Lucheng district under different daily precipitation conditions. The areas (a–e) depict the distribution maps of flood risk assessments under daily precipitation conditions of 403.8 mm, 350 mm, 250 mm, 150 mm, and 50 mm.

From Figure 7, it can be seen that precipitation is an important factor in changing the flood disaster level in the Lucheng district. (1) In the Lucheng District, a medium-risk area with a relatively low risk of flooding, the comprehensive index value of flood assessment is higher than 0.75 when the day precipitation is 50 mm. However, Guanghua Street and Wuma Street have comprehensive index values close to 0.75, indicating a high level of risk. (2) As the precipitation intensifies, the comprehensive flood disaster index for the three streets—Binjiang, Danan, and Puxie—begins to decline below 0.50, indicating that the risk level in the area above has increased to that of a greater risk area. The remaining streets are still in a medium-risk area. (3) Six areas (Binjiang, Puxie, Nanhui, Danan, Nanjiao, and Songtai) will have a greater danger of flooding when the precipitation continues to rise to 250 mm. (4) However, it could be found that the distribution of flood catastrophe risk areas remains the same as the precipitation continues to rise, reaching 350 mm or even 403.88 mm. The following six streets are the highest-risk locations, while Wuma Street and Guanghua Street remain medium-risk zones.

In summary, varied rainfall conditions will affect how well each street in Wenzhou’s Lucheng area can handle flood disasters. While Binjiang, Puxue, and Danan are more susceptible, Guanghua and Wuma are the best among them, followed by Nanhui, Nanjiao, and Songtai. Despite the remarkable achievements of this study, it is important to acknowledge the following limitations: this research primarily conducted flood risk assessment based on current environmental and climatic conditions, yet it did not fully consider potential

future changes, such as climate change and accelerated urbanization. These factors may significantly impact flood disaster risks and warrant further exploration in future studies.

A comparative analysis was conducted to further validate the model's reliability between the region's risk index of rainstorms and flood disasters from 1987 to 2022 and the disaster grade during the same period (Figure 8). The results revealed a strong correlation between the risk index and the total disaster grade, with a correlation coefficient of 0.8837, reaching a significant level. This indicates that the evaluation indicators are highly accurate. This also indirectly confirms the applicability of the AHP and the entropy method.

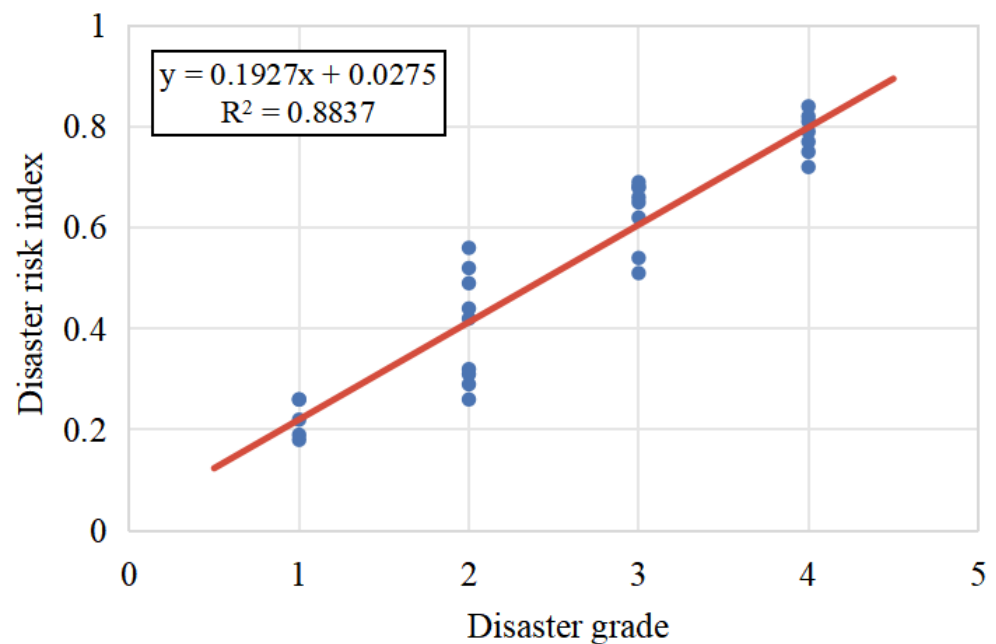


**Figure 8.** Accuracy test of flood disaster risk index. The disaster grade in the figure is divided into four levels: 1, 2, 3, and 4, with level 1 being the most severe and level 4 being the least severe.

Flood disaster management in coastal plain river network areas requires integrating various flood risk management measures to help reduce urban flood risks. These measures can be primarily categorized into engineering measures and non-engineering measures. Engineering measures aim to decrease flood risks by controlling water inflow outside urban residential areas. Non-engineering measures focus on ensuring safety through optimizing urban development planning and management. The two complement each other. Comprehensive strategies should be integrated with existing urban planning and management policies and practices. Furthermore, engineering and non-engineering measures are not mutually exclusive; optimized urban flood management often necessitates the combination of both. Additionally, it is essential to understand the extent and characteristics of existing risks and potential future changes in risks to achieve a balance between short-term and long-term investments in integrated flood risk management. With the acceleration of urbanization and climate change, there is a need to shift from the current over-reliance on engineering flood control infrastructure to more adaptive non-engineering solutions.

## 5. Conclusions

This study conducted a systematic flood risk assessment targeting coastal plain cities, taking Lucheng District in Wenzhou City, Zhejiang Province, as an example. A quantitative assessment of flood disaster risks in typical plain river network areas was carried out by establishing a set of flood disaster evaluation index systems adapted to environmental changes, combining subjective and objective weighting methods, and introducing a fuzzy matter-element model based on correlation degree. Further analysis was conducted on the

distribution of flood disaster risks in Lucheng District under different daily precipitation conditions. The conclusions are as follows:

(1) Regarding hazard-inducing factors, Lucheng District is primarily influenced by precipitation amount and duration. As precipitation increases, flood disaster risks rise in some street areas, but the overall risk level remains stable. Regarding the disaster-forming environment, factors such as topography, river network density, and vegetation cover significantly impact flood disaster risks in Lucheng District. The study found that areas with higher river network density generally have lower flood risks, while low-lying areas and those with sparse river networks have higher risks. Regarding disaster-bearing bodies, factors such as population density and economic development level in Lucheng District affect flood disaster risks. However, compared to hazard-inducing factors and the disaster-forming environment, the differences in disaster-bearing bodies among different street areas in Lucheng District are relatively small, with limited impact on the overall risk level.

(2) Five different daily precipitation scenarios (50 mm, 150 mm, 250 mm, 350 mm, 403.8 mm) were set, and flood disaster risk assessment maps were created using ArcGIS software (version 10.8). The results indicate that as precipitation increases, the flood disaster risk level rises in some street areas of Lucheng District, but the overall risk level remains within a moderate range.

(3) By comparing flood disaster risk indices with concurrent disaster levels, it was demonstrated that the flood disaster evaluation index system constructed through integrating GIS technology with flood forecasting models, numerical simulations, and spatial analysis techniques possesses strong reliability and accuracy.

In summary, the quantitative assessment of flood disaster risks in Lucheng District provides a scientific basis for local governments and relevant departments to formulate flood control and disaster reduction measures. The flood disaster evaluation index system and calculation framework developed in this study have important guiding significance for flood risk assessments in coastal plain cities.

**Author Contributions:** Conceptualization, S.H. and H.C.; methodology, W.X.; software, H.Q.; validation, J.Y.; formal analysis, X.C.; investigation, H.C.; resources, H.N.; data curation, H.Q.; writing—original draft preparation, W.X.; writing—review and editing, H.C.; visualization, S.H.; supervision, H.C.; project administration, S.H.; funding acquisition, H.C. All authors have read and agreed to the published version of the manuscript.

**Funding:** This research was funded by the Zhejiang Provincial Natural Science Foundation, grant number ZCLQ24E0901 and LZJWY22E090007; the Scientific Research Fund of Zhejiang Provincial Education Department, grant number Y202352492; the Huzhou Science and Technology Plan Project, grant number 2023GZ64; the Zhejiang Provincial Water Resources Department Science and Technology Program, grant number RC2213.

**Data Availability Statement:** The data presented in this study are available on request from the corresponding author.

**Acknowledgments:** We are grateful to the Wenzhou Bureau of Hydrology and Water Resources for providing hydrological and meteorological data.

**Conflicts of Interest:** The authors declare no conflicts of interest.

## References

1. Lyu, H.-M.; Yin, Z.-Y.; Zhou, A.; Shen, S.-L. MCDM-Based Flood Risk Assessment of Metro Systems in Smart City Development: A Review. *Environ. Impact Assess. Rev.* **2023**, *101*, 107154. [[CrossRef](#)]
2. Rosmadi, H.S.; Ahmed, M.F.; Mokhtar, M.B.; Lim, C.K. Reviewing Challenges of Flood Risk Management in Malaysia. *Water* **2023**, *15*, 2390. [[CrossRef](#)]
3. Lagmay, A.M.F.A.; Racoma, B.A.; Aracan, K.A.; Alconis-Ayco, J.; Saddi, I.L. Disseminating Near-Real-Time Hazards Information and Flood Maps in the Philippines through Web-GIS. *J. Environ. Sci.* **2017**, *59*, 13–23. [[CrossRef](#)]
4. Ding, Y.; Wang, H.; Liu, Y.; Lei, X. Urban Waterlogging Structure Risk Assessment and Enhancement. *J. Environ. Manag.* **2024**, *352*, 120074. [[CrossRef](#)]

5. Huang, Y.; Lin, J.; He, X.; Lin, Z.; Wu, Z.; Zhang, X. Assessing the Scale Effect of Urban Vertical Patterns on Urban Waterlogging: An Empirical Study in Shenzhen. *Environ. Impact Assess. Rev.* **2024**, *106*, 107486. [[CrossRef](#)]
6. Chen, H.; Huang, S.; Xu, Y.-P.; Teegavarapu, R.S.V.; Guo, Y.; Nie, H.; Xie, H. Using Baseflow Ensembles for Hydrologic Hysteresis Characterization in Humid Basins of Southeastern China. *Water Resour. Res.* **2024**, *60*, e2023WR036195. [[CrossRef](#)]
7. Rashid, M.B. Monitoring of Drainage System and Waterlogging Area in the Human-Induced Ganges-Brahmaputra Tidal Delta Plain of Bangladesh Using MNDWI Index. *Heliyon* **2023**, *9*, e17412. [[CrossRef](#)]
8. Shi, B.; Zhang, R. Sensitivity Analysis and Optimization Scheme of Waterlogging Control Measures in a Coastal Plain of Wenzhou. In *Advances in Urban Construction and Management Engineering*; CRC Press: Boca Raton, FL, USA, 2023; ISBN 978-1-00-334802-3.
9. Rashid, M.B.; Sheikh, M.R.; Haque, A.J.M.E.; Patwary, M.A.A.; Siddique, M.A.B.; Habib, M.A.; Sarker, M.N. Consequences of Catastrophic Cyclone Amphan in the Human-Induced Coastal Plain Ecosystems of Bangladesh. *Case Stud. Chem. Environ. Eng.* **2023**, *8*, 100467. [[CrossRef](#)]
10. Guo, Y.; Xu, Y.-P.; Yu, X.; Liu, L.; Gu, H. AI-based ensemble flood forecasts and its implementation in multi-objective robust optimization operation for reservoir flood control. *Water Resour. Res.* **2024**, *60*, e2023WR035693. [[CrossRef](#)]
11. Liu, Y.; Chen, B.; Duan, C.; Wang, H. Economic Loss of Urban Waterlogging Based on an Integrated Drainage Model and Network Environ Analyses. *Resour. Conserv. Recycl.* **2023**, *192*, 106923. [[CrossRef](#)]
12. Prashar, N.; Lakra, H.S.; Shaw, R.; Kaur, H. Urban Flood Resilience: A Comprehensive Review of Assessment Methods, Tools, and Techniques to Manage Disaster. *Prog. Disaster Sci.* **2023**, *20*, 100299. [[CrossRef](#)]
13. Zhang, Y.; Yue, W.; Su, M.; Teng, Y.; Huang, Q.; Lu, W.; Rong, Q.; Xu, C. Assessment of Urban Flood Resilience Based on a Systematic Framework. *Ecol. Indic.* **2023**, *150*, 110230. [[CrossRef](#)]
14. Rezende, O.M.; Miranda, F.M.; Haddad, A.N.; Miguez, M.G. A Framework to Evaluate Urban Flood Resilience of Design Alternatives for Flood Defence Considering Future Adverse Scenarios. *Water* **2019**, *11*, 1485. [[CrossRef](#)]
15. Hammond, M.; Chen, A.S.; Batica, J.; Butler, D.; Djordjević, S.; Gourbesville, P.; Manojlović, N.; Mark, O.; Veerbeek, W. A New Flood Risk Assessment Framework for Evaluating the Effectiveness of Policies to Improve Urban Flood Resilience. *Urban Water J.* **2018**, *15*, 427–436. [[CrossRef](#)]
16. Chen, J.; Li, Q.; Wang, H.; Deng, M. A Machine Learning Ensemble Approach Based on Random Forest and Radial Basis Function Neural Network for Risk Evaluation of Regional Flood Disaster: A Case Study of the Yangtze River Delta, China. *Int. J. Environ. Res. Public Health* **2019**, *17*, 49. [[CrossRef](#)]
17. Zhu, Z.; Zhang, Y. Flood Disaster Risk Assessment Based on Random Forest Algorithm. *Neural Comput. Appl.* **2022**, *34*, 3443–3455. [[CrossRef](#)]
18. Kulawiak, M.; Prospathopoulos, A.; Perivoliotis, L.; Luba, M.; Kioroglou, S.; Stepnowski, A. Interactive Visualization of Marine Pollution Monitoring and Forecasting Data via a Web-Based GIS. *Comput. Geosci.* **2010**, *36*, 1069–1080. [[CrossRef](#)]
19. Mohanty, M.P.; Karmakar, S. WebFRIS: An Efficient Web-Based Decision Support Tool to Disseminate End-to-End Risk Information for Flood Management. *J. Environ. Manag.* **2021**, *288*, 112456. [[CrossRef](#)]
20. Miranda, F.; Franco, A.B.; Rezende, O.; da Costa, B.B.F.; Najjar, M.; Haddad, A.N.; Miguez, M. A GIS-Based Index of Physical Susceptibility to Flooding as a Tool for Flood Risk Management. *Land* **2023**, *12*, 1408. [[CrossRef](#)]
21. Efraimidou, E.; Spiliotis, M. A GIS-Based Flood Risk Assessment Using the Decision-Making Trial and Evaluation Laboratory Approach at a Regional Scale. *Environ. Process.* **2024**, *11*, 9. [[CrossRef](#)]
22. Taherizadeh, M.; Niknam, A.; Nguyen-Huy, T.; Mezósi, G.; Sarli, R. Flash Flood-Risk Areas Zoning Using Integration of Decision-Making Trial and Evaluation Laboratory, GIS-Based Analytic Network Process and Satellite-Derived Information. *Nat. Hazards* **2023**, *118*, 2309–2335. [[CrossRef](#)]
23. Doorga, J.R.S.; Magerl, L.; Bunwaree, P.; Zhao, J.; Watkins, S.; Staub, C.G.; Rughooputh, S.D.D.V.; Cunden, T.S.M.; Lollchund, R.; Boojhawon, R. GIS-Based Multi-Criteria Modelling of Flood Risk Susceptibility in Port Louis, Mauritius: Towards Resilient Flood Management. *Int. J. Disaster Risk Reduct.* **2022**, *67*, 102683. [[CrossRef](#)]
24. Ahmad, I.; Wang, X.; Waseem, M.; Zaman, M.; Aziz, F.; Khan, R.Z.N.; Ashraf, M. Flood Management, Characterization and Vulnerability Analysis Using an Integrated RS-GIS and 2D Hydrodynamic Modelling Approach: The Case of Deg Nullah, Pakistan. *Remote Sens.* **2022**, *14*, 2138. [[CrossRef](#)]
25. Peker, İ.B.; Gülbaz, S.; Demir, V.; Orhan, O.; Beden, N. Integration of HEC-RAS and HEC-HMS with GIS in Flood Modeling and Flood Hazard Mapping. *Sustainability* **2024**, *16*, 1226. [[CrossRef](#)]
26. Endendijk, T.; Botzen, W.J.W.; de Moel, H.; Aerts, J.C.J.H.; Slager, K.; Kok, M. Flood Vulnerability Models and Household Flood Damage Mitigation Measures: An Econometric Analysis of Survey Data. *Water Resour. Res.* **2023**, *59*, e2022WR034192. [[CrossRef](#)]
27. Amirmoradi, K.; Shokoohi, A. River Flash Flood Economical Loss and Its Uncertainty in Developing Countries. *Water Resour. Manag.* **2024**, *38*, 81–105. [[CrossRef](#)]
28. Popandopulo, G.; Illarionova, S.; Shadrin, D.; Evteeva, K.; Sotiriadi, N.; Burnaev, E. Flood Extent and Volume Estimation Using Remote Sensing Data. *Remote Sens.* **2023**, *15*, 4463. [[CrossRef](#)]
29. Haselbach, L.; Adesina, M.; Muppavarapu, N.; Wu, X. Spatially Estimating Flooding Depths from Damage Reports. *Nat. Hazards* **2023**, *117*, 1633–1645. [[CrossRef](#)]
30. Zalnezhad, A.; Rahman, A.; Ahamed, F.; Vafakhah, M.; Samali, B. Design Flood Estimation at Ungauged Catchments Using Index Flood Method and Quantile Regression Technique: A Case Study for South East Australia. *Nat. Hazards* **2023**, *119*, 1839–1862. [[CrossRef](#)]

31. Zellou, B.; Rahali, H. Assessment of the Joint Impact of Extreme Rainfall and Storm Surge on the Risk of Flooding in a Coastal Area. *J. Hydrol.* **2019**, *569*, 647–665. [[CrossRef](#)]
32. Li, Y.; Gao, J.; Yin, J.; Wu, S. Assessing the Potential of Compound Extreme Storm Surge and Precipitation along China's Coastline. *Weather. Clim. Extrem.* **2024**, *45*, 100702. [[CrossRef](#)]
33. Feng, J.; Li, D.; Li, Y.; Zhao, L. Analysis of Compound Floods from Storm Surge and Extreme Precipitation in China. *J. Hydrol.* **2023**, *627*, 130402. [[CrossRef](#)]
34. Wang, H.; Xuan, Y.; Tran, T.V.T.; Couasonon, A.; Scussolini, P.; Luu, L.N.; Nguyen, H.Q.; Reeve, D.E. Changes in Seasonal Compound Floods in Vietnam Revealed by a Time-Varying Dependence Structure of Extreme Rainfall and High Surge. *Coast. Eng.* **2023**, *183*, 104330. [[CrossRef](#)]
35. Li, G.; Wu, X.; Han, J.-C.; Li, B.; Huang, Y.; Wang, Y. Flood Risk Assessment by Using an Interpretative Structural Modeling Based Bayesian Network Approach (ISM-BN): An Urban-Level Analysis of Shenzhen, China. *J. Environ. Manag.* **2023**, *329*, 117040. [[CrossRef](#)]
36. Wang, Y.; Zhang, Q.; Lin, K.; Liu, Z.; Liang, Y.; Liu, Y.; Li, C. A Novel Framework for Urban Flood Risk Assessment: Multiple Perspectives and Causal Analysis. *Water Res.* **2024**, *256*, 121591. [[CrossRef](#)]
37. Roperio, R.F.; Flores, M.J.; Rumí, R. Flash Floods in Mediterranean Catchments: A Meta-Model Decision Support System Based on Bayesian Networks. *Environ. Ecol. Stat.* **2024**, *31*, 27–56. [[CrossRef](#)]
38. Ma, Y.; Wang, Z.; Xiong, Y.; Yuan, W.; Wang, Y.; Tang, H.; Zheng, J.; Liu, Z. A Critical Application of Different Methods for the Vulnerability Assessment of Shallow Aquifers in Zhengzhou City. *Environ. Sci. Pollut. Res.* **2023**, *30*, 97078–97091. [[CrossRef](#)]
39. Ayan, B.; Abacıoğlu, S.; Basilio, M.P. A Comprehensive Review of the Novel Weighting Methods for Multi-Criteria Decision-Making. *Information* **2023**, *14*, 285. [[CrossRef](#)]
40. Singh, T.; Singh, V.; Ranakoti, L.; Kumar, S. Optimization on Tribological Properties of Natural Fiber Reinforced Brake Friction Composite Materials: Effect of Objective and Subjective Weighting Methods. *Polym. Test.* **2023**, *117*, 107873. [[CrossRef](#)]
41. Ji, Y.; Gao, D.; Liu, Q.; Su, J.; Liu, Y.; Zhao, J.; Yang, Y.; Fu, Y.; Huang, G. An Integrated Framework for Agricultural Non-Point Source Pollution Control Technology Evaluation: Application of an Improved Multiple Attribute Decision Making Method. *Expert Syst. Appl.* **2023**, *229*, 120319. [[CrossRef](#)]
42. Zhao, J.; Jin, J.; Zhu, J.; Xu, J.; Hang, Q.; Chen, Y.; Han, D. Water Resources Risk Assessment Model Based on the Subjective and Objective Combination Weighting Methods. *Water Resour. Manag.* **2016**, *30*, 3027–3042. [[CrossRef](#)]
43. Kumar, A.; Abirami, S. Aspect-Based Opinion Ranking Framework for Product Reviews Using a Spearman's Rank Correlation Coefficient Method. *Inform. Sci.* **2018**, *460–461*, 23–41. [[CrossRef](#)]
44. Chen, H.; Xu, Z.; Liu, Y.; Huang, Y.; Yang, F. Urban Flood Risk Assessment Based on Dynamic Population Distribution and Fuzzy Comprehensive Evaluation. *Int. J. Environ. Res. Public Health* **2022**, *19*, 16406. [[CrossRef](#)]
45. Ma, L.; Chen, H.; Yan, H.; Li, W.; Zhang, J.; Zhang, W. Post Evaluation of Distributed Energy Generation Combining the Attribute Hierarchical Model and Matter-Element Extension Theory. *J. Clean. Prod.* **2018**, *184*, 503–510. [[CrossRef](#)]
46. Ren, D.; Song, Y.; Wang, X. Evaluation and Computation of University Emergency Management Ability Based on AHP and Matter Element Extension Model. In Proceedings of the 2023 IEEE 3rd International Conference on Social Sciences and Intelligence Management (SSIM), Taichung, Taiwan, 15–17 December 2023; pp. 153–158.
47. Wang, Q.; Yang, J.; Li, Z.; Xiao, Y.; Jia, C.; Chen, H.; Chen, H. Evaluation System of Substation Based on AHP-EWM and Matter-Element Extension Theory. In Proceedings of the 2023 IEEE Sustainable Power and Energy Conference (ISPEC), Chongqing, China, 29–30 November 2023; pp. 1–6.
48. Albahri, O.S.; Alamoodi, A.H.; Deveci, M.; Albahri, A.S.; Mahmoud, M.A.; Sharaf, I.M.; Coffman, D. Multi-Perspective Evaluation of Integrated Active Cooling Systems Using Fuzzy Decision Making Model. *Energy Policy* **2023**, *182*, 113775. [[CrossRef](#)]
49. Yamagishi, K.; Gantalao, C.; Tiu, A.M.; Tanaid, R.A.; Medalla, M.E.; Abellana, D.P.; Egberto Selerio, J.; Ocampo, L. Evaluating the Destination Management Performance of Small Islands with the Fuzzy Best-Worst Method and Fuzzy Simple Additive Weighting. *Curr. Issues Tour.* **2023**, *26*, 1224–1253. [[CrossRef](#)]
50. Zhu, D.; Li, Z.; Mishra, A.R. Evaluation of the Critical Success Factors of Dynamic Enterprise Risk Management in Manufacturing SMEs Using an Integrated Fuzzy Decision-Making Model. *Technol. Forecast. Soc.* **2023**, *186*, 122137. [[CrossRef](#)]
51. Li, G.; Zhang, C.; Huo, Z. Reconciling Crop Production and Ecological Conservation under Uncertainty: A Fuzzy Credibility-Based Multi-Objective Simulation-Optimization Model. *Sci. Total Environ.* **2023**, *873*, 162340. [[CrossRef](#)]
52. Chemkomnerd, N.; Pannakkong, W.; Tanantong, T.; Huynh, v.-N.; Karnjana, J. A Simulation-Based Multi-Objective Optimization Framework to Enhance Patient Satisfaction: A Case Study of Ophthalmology Department Management. *IEEE Access* **2024**, *12*, 93197–93220. [[CrossRef](#)]
53. Boru İpek, A. Multi-Objective Simulation Optimization Integrated With Analytic Hierarchy Process and Technique for Order Preference by Similarity to Ideal Solution for Pollution Routing Problem. *Transp. Res. Rec. J. Transp. Res. Board* **2023**, *2677*, 1658–1674. [[CrossRef](#)]
54. Dehghanimohammadabadi, M.; Rezaeiahari, M.; Seif, J. Multi-Objective Patient Appointment Scheduling Framework (MO-PASS): A Data-Table Input Simulation–Optimization Approach. *Simulation* **2022**, *99*, 363–383. [[CrossRef](#)]
55. Mirjalili, S.; Jangir, P.; Saremi, S. Multi-Objective Ant Lion Optimizer: A Multi-Objective Optimization Algorithm for Solving Engineering Problems. *Appl. Intell.* **2017**, *46*, 79–95. [[CrossRef](#)]

56. Ghera, F.; Figarola, L.A.; Castro, R.; Ferraro, D.O. AgrOptim: A Novel Multi-Objective Simulation Optimization Framework for Extensive Cropping Systems. *Comput. Electron. Agric.* **2024**, *224*, 109119. [[CrossRef](#)]
57. Li, W.; Wang, L.; Ye, Z.; Liu, Y.; Wang, Y. A Dynamic Combination Algorithm Based Scenario Construction Theory for Mine Water-Inrush Accident Multi-Objective Optimization. *Expert Syst. Appl.* **2024**, *238*, 121871. [[CrossRef](#)]
58. Yue, Q.; Cui, N.; Zhang, F.; Guo, S.; Jiang, S.; Yu, X.; Zhu, B. Adaptation to Seasonal Drought in Irrigation Districts of South China: A Copula-Based Fuzzy-Flexible Stochastic Multi-Objective Approach for Precise Irrigation Planning. *J. Hydrol.* **2023**, *625*, 129986. [[CrossRef](#)]

**Disclaimer/Publisher's Note:** The statements, opinions and data contained in all publications are solely those of the individual author(s) and contributor(s) and not of MDPI and/or the editor(s). MDPI and/or the editor(s) disclaim responsibility for any injury to people or property resulting from any ideas, methods, instructions or products referred to in the content.